

## Superconducting Fluxon Pumps and Lenses

J. F. Wambaugh,<sup>1</sup> C. Reichhardt,<sup>2</sup> C. J. Olson,<sup>2</sup> F. Marchesoni,<sup>1,3</sup> and Franco Nori<sup>1,\*</sup>

<sup>1</sup>Department of Physics, The University of Michigan, Ann Arbor, Michigan 48109-1120

<sup>2</sup>Physics Department, University of California, Davis, California 95616

<sup>3</sup>Istituto Nazionale di Fisica della Materia, Università di Camerino, Camerino I-62032, Italy

(Received 29 July 1999)

We study stochastic transport of fluxons in superconductors by alternating current (ac) rectification. Our simulated system provides a fluxon pump, “lens,” or fluxon “rectifier” because the applied electrical ac is transformed into a net dc motion of fluxons. Thermal fluctuations and the asymmetry of the ratchet channel walls induce this “diode” effect, which can have important applications in devices, such as SQUID magnetometers, and for fluxon optics, including convex and concave fluxon lenses. Certain features are unique to this novel two-dimensional (2D) geometric pump, and different from the previously studied 1D ratchets.

PACS numbers: 74.60.Ge, 05.40./hskip1pt–/hskip1pta, 05.60./hskip1pt–/hskip1ptk

A number of authors (see, e.g., [1–4]) have recently addressed the long-standing problem of how to extract useful work from a fluctuating environment. While heat may not be transformed back to mechanical work at thermal equilibrium (i.e., without temperature gradients [5]), the same restriction does not apply to the case of nonequilibrium thermal fluctuations: An asymmetric device (such as Feynman’s ratchet [5]) can indeed rectify symmetric quasiequilibrium fluctuations [1–4]. The implications of such a mechanism in transport theory are far reaching: macroscopic currents may arise even in the absence of external forces or gradients.

Recently, a few groups [6,7] have made interesting proposals for quite distinct ways of using ratchets in superconductors. Reference [6] uses Josephson junctions, in SQUIDs and arrays, while Ref. [7] uses a *standard 1D* potential-energy ratchet (e.g., [1,3,4]) to drive fluxons out of superconducting samples using simulations as in [8,9]. Here, we use the new concept of *2D asymmetric channel walls* to provide an experimentally realizable way to easily move fluxons through channels in ac-driven devices. These novel *geometric ratchets* would allow, for example, the construction of *fluxon optics* devices, including concave/convex fluxon *lenses* that disperse/concentrate fluxons in nanodevices. Further, we also consider the effects of *collective* interactions on ratchets, instead of the usual *one-particle* stochastic transport.

*Simulation.*—Computer simulations were performed using a new version of the molecular dynamics (MD) code used for systems with random [8] and correlated [9] pinning. We model a transverse 2D slice (in the  $x$ - $y$  plane) of an infinite zero-field-cooled superconducting slab containing current-driven 3D rigid vortices that are parallel to the sample edge. The samples have very strong, effectively infinite, pinning except the “zero pinning” *central sawtooth-shaped channel* (see inset of Fig. 1). In the latter, fluxons moved subject to fluxon-fluxon repulsions  $\mathbf{f}_{vv}$ , an externally applied ac Lorentz driving force  $\mathbf{f}_L$ , forces due to thermal fluctuations  $\mathbf{f}_T$ , and interactions with the chan-

nel boundaries, treated as infinite potential barriers. The thermal force  $\mathbf{f}_T$  was implemented using a Box-Muller zero-mean, Gaussian distributed random number generator. We measure all forces in units of  $f_0 = \Phi_0^2/8\pi^2\lambda^3$ , magnetic fields in units of  $\Phi_0/\lambda^2$ , and lengths in units of the penetration depth  $\lambda$ . Here,  $\Phi_0 = hc/2e$  is the flux quantum. Our dimensionless temperature is  $T = k_B T_{\text{actual}}/\lambda f_0$ . Thus, away from the channel edge, the total force on a fluxon is  $\mathbf{f} = \mathbf{f}_{vv} + \mathbf{f}_L + \mathbf{f}_T = \eta \mathbf{v}$ , where the total force on vortex  $i$  due to other vortices is given by  $\mathbf{f}_{vv}^{(i)} = \sum_{j=1}^{N_v} f_0 K_1(|\mathbf{r}_i - \mathbf{r}_j|/\lambda) \hat{\mathbf{r}}_{ij}$ . Here,  $K_1$  is a modified Bessel function,  $\mathbf{r}_i$  ( $\mathbf{v}_i$ ) is the location (velocity) of the  $i$ th vortex,  $N_v$  is the number of vortices,  $\hat{\mathbf{r}}_{ij} = (\mathbf{r}_i - \mathbf{r}_j)/|\mathbf{r}_i - \mathbf{r}_j|$ , and we take  $\Delta t = 0.01$  and  $\eta = 1$ . Simulations for the same parameters were repeated with different random number seeds, to provide for disorder averaging.

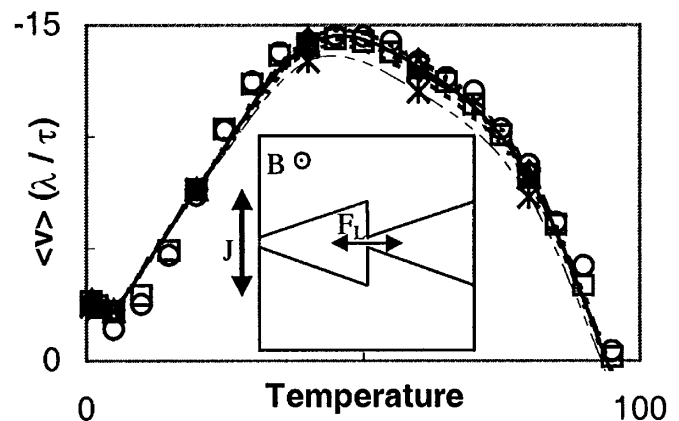


FIG. 1. Rectified average fluxon velocity  $\langle v \rangle$ , which can be measured as a voltage, versus temperature  $T$  for the ratchet geometry in the inset. The magnetic field  $B$  is directed out of the figure.  $\mathbf{J} = J\hat{\mathbf{y}}$  is a vertically applied alternating current square wave that drives the fluxons back and forth horizontally along the channel. The number of fluxons is as follows: 1 ( $\circ$ ), 25 ( $\diamond$ ), 50 ( $\square$ ), 75 ( $\triangle$ ), 100 ( $\times$ ), 150 ( $+$ ), 250 ( $*$ ).

Unless otherwise specified, each figure refers to simulations conducted in the following way: Initially fluxons were randomly placed inside the channel and subjected to an alternating current along  $y$ —producing a square-wave Lorentz driving force along  $x$  with  $F \equiv f_L/f_0 = 15$  and period  $P = 2\tau$  (here,  $\tau = 100$  MD steps). This means that in the absence of thermal noise ( $T = 0$ ) and channel walls, a single fluxon would alternate traveling  $15\lambda$  in one direction (e.g.,  $+x$ ), and then  $15\lambda$  in the other ( $-x$ ). The period  $9\lambda$  of the horizontal ratchet teeth was such that the driving force  $F = 15$  should be sufficient to allow for a rectification, or diode effect, because it moves the fluxon back and forth through the bottlenecks indicated in the inset of Fig. 1. Ten runs, of 250 000 MD steps each, were used to find the average current and standard deviation for each plotted point. When a standard deviation is not shown, it was significantly smaller than the plotted point. All samples had a 2D geometric ratchet made of asymmetric walls. The simulated sample was an  $18\lambda$  by  $18\lambda$  square, with periodic boundary conditions. The channel is  $7\lambda$  wide, with sawteeth of period  $9\lambda$  (four teeth per unit cell) and slope  $1/3$  [except in Fig. 5 (below), and in other runs to be discussed elsewhere, where geometry was varied]. This leads to a bottleneck that is  $1\lambda$  wide. This construction is a novel 2D ratchet that uses geometry, which governs the system potential energy, to cause rectification.

*Temperature dependence of the fluxon rectification.*—Figure 1 shows the rectified fluxon velocity  $\langle v \rangle = \sum_i^{N_v} v_i / N_v$  versus temperature. The dimensionless temperature  $T$  was varied over 2 orders of magnitude, from 1 to 100. These simulations clearly indicate an optimal or “resonant” temperature regime in which the dc fluxon velocity is maximized by the fluxon pump or diode. This optimal temperature regime can be explained as a trade-off between allowing the fluxons to fully explore the ratchet geometry (i.e.,  $T$  must not be too low) and washing out the driving force (i.e.,  $T$  must not be too large). At low temperatures, the alternating driving force will cause a fluxon to migrate to the center of the channel and no longer be impeded or assisted by interactions with the geometry; while at high temperatures the driving force becomes irrelevant and thus the fluxon is no longer pushed through bottlenecks regularly. The  $\langle v \rangle(T)$  curve for many randomly placed fluxons is similar to the single fluxon case, but the magnitude of  $\langle v \rangle(T)$  decreases when the fluxon density  $B$  increases. This is because the repulsive force produced by a large number of fluxons acts to restrict each other’s motion. Note that, at the optimal temperature, the fluxons travel nearly  $15\lambda$  every 100 MD steps. The general shape of the curve was established with two fine scans with one and fifty fluxons. Conformity of other field strengths to this curve was judged by performing a coarser scan, then connecting the points with a spline. The small dip in the  $\langle v \rangle$  for low  $T$  will be discussed separately (see Fig. 3 below).

*Driving period dependence of the flux pump.*—Figure 2(a) shows  $\langle v \rangle(P)$  for six different combinations of driving force amplitudes  $F$  and temperatures  $T$  for a single fluxon. Interestingly, as the period  $P$  of the driving force was varied from low to high (from  $P = 20$  MD steps to 2000 MD steps) *no optimal peak* in  $\langle v \rangle$  was discovered. This is in contrast with previous work on ratchets, which provide a peak in  $\langle v \rangle$  versus either  $P$  or frequency. Instead, we find that, while a high frequency driving force yields a very small ratchet velocity, the velocity quickly converges to a nearly stable value with increasing  $P$ . This result corresponds to the idea that a fluxon must be forced through the bottleneck of the geometric 2D ratchet in order for it to be a rectifier. At high frequencies, a fluxon does not travel far enough to interact with the bottleneck. Once the frequency is low enough to force it through a bottleneck, however, the net velocity changes little by forcing it through further bottlenecks.

All of the simulations in Fig. 2(a) were conducted at relatively low temperatures to allow the effects of the driving force to dominate. In addition to trying

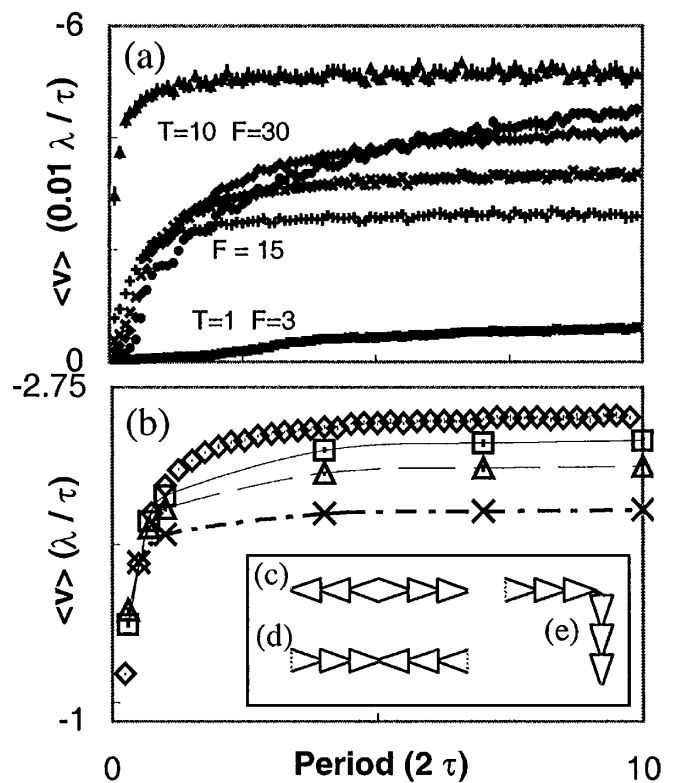


FIG. 2. Average fluxon velocity  $\langle v \rangle$  versus driving force period  $P$  for (a) one fluxon and (b) many fluxons. For very low periods, little rectification occurs and, for higher periods,  $\langle v \rangle$  slowly increases. The four  $F = 15$  curves in the middle of (a) show similar behavior and correspond to the following (top to bottom at  $\tau = 10$ ):  $T = 1$  ( $\bullet$ ),  $T = 2$  ( $\diamond$ ),  $T = 3$  ( $\times$ ),  $T = 10$  ( $+$ ). In (b), similar  $\langle v \rangle$  occur for 50 ( $\diamond$ ), 100 ( $\square$ ), 150 ( $\triangle$ ), and 250 ( $\times$ ) fluxons. Inset: Schematic diagram for concave (c) and convex (d) fluxon lenses that disperse/focus fluxons from/at their centers. (e) shows a corner unit.

$F = f_L/f_0 = 15$ , the value typically used in this paper, two combinations of driving force and temperature magnitudes were tried that both also had an  $F/T$  ratio of 3/1. While varying  $P$  at the low- $T$  regime had little effect upon the period dependence curve, varying  $F$  very clearly did have an effect: the higher  $F$ , the greater  $\langle v \rangle$ .

Figure 2(b) shows the dependence of  $\langle v \rangle$  on  $P$ , for  $T = F/3 = 5$  with many fluxons instead of one. Initially, 50 randomly placed fluxons were simulated. As with the single fluxon case, a high frequency driving force resulted in a low  $\langle v \rangle$  because the fluxons were not being forced through the ratchet bottleneck. Increasing  $P$  produced a rapidly plateauing  $\langle v \rangle$ . Once the shape of the curve was determined, similar sets of observations were made of different fluxon densities  $B$  at six different periods. These simulations of many fluxons demonstrate that, as with one fluxon, there was *no* optimal peak.

*Fluxon pump effect versus field.*—By varying the density of fluxons  $B$ , we found a maximum in  $\langle v \rangle$  at very low temperatures (see Fig. 3). This is due to an enhanced interaction with the ratchet geometry: at extremely low  $T$  the driven fluxons eventually work their way to the middle of the channel and then no longer interact with the ratchet. A small increase in  $B$  can drive fluxons from the middle of the channel, causing these fluxons to increase their interaction with the sawteeth, without significantly increasing the resistance due to fluxon-fluxon interactions. Aside from this low- $T$  resonance, increasing  $B$  slowly decreases  $\langle v \rangle$ , because, as the fluxons repel one another, at high densities they *block* the bottleneck. At high temperatures (e.g.,  $T = 50$ ) the ratchet velocity decreases slowly with increased fluxons. In this case, the slight maximum in  $\langle v \rangle$  found at low  $T$  is not present because the resistance due to fluxon-fluxon interactions is always larger than the gains from increased exploration of the geometry of the ratchet.

*Flux pump response to the driving force.*—Increasing the amplitude  $F$  of the square-wave driving force increases the average velocity  $\langle v \rangle$  of a fluxon in the ratchet, as shown in Fig. 4. This monotonic increase in  $\langle v \rangle$  versus  $F$  for 2D

geometric ratchets is different from the peak observed in 1D potential ratchets (e.g., see Fig. 2 of [7]). This makes it fairly easy for any particular 2D geometric ratchet to be continuously tuned to desired values of  $\langle v \rangle$ . This would be an advantage of 2D geometrical over 1D potential ratchets for potential practical designs of devices. A reason for their different response is because the resistance to motion due to successive bottlenecks does not add like the resistance due to successive potential barriers. If a fluxon happens to remain for some time in the center of a bottleneck, unlikely to happen at high enough temperatures, then it will not be rectified; while the potential barrier rectifies at every period. Increased fluxon density again increases resistance, reducing  $\langle v \rangle$ .

*Geometry dependence.*—To determine the generality of the simulation results presented here with respect to varied ratchet geometries, in Fig. 5 we compare  $\langle v \rangle(T)$  for 50 fluxons in two alternate geometries with the  $\langle v \rangle(T)$  shown in Fig. 1 (open squares in both figures). Increasing the slope, and correspondingly decreasing the period, of the sawteeth clearly shifts the optimal temperature to lower values. Despite this shift, however, the qualitative behavior of the first geometry studied carried over to other ratchet slopes and periods. Additional samples and parameters, including wider bottlenecks, were also studied (but not discussed here due to space limitations), giving consistent results.

*Discussion.*—Our 2D geometric ratchet has some properties which are similar to previously studied 1D potential ratchets. Like the simpler 1D cases, the 2D ratchet showed a “resonance region” with a maximum in  $\langle v \rangle$ , and (outside of a low- $T$  anomaly) a decreased  $\langle v \rangle$  with increasing  $B$ . Unlike the 1D cases, however, the ratchet velocity plateaus with decreased driving frequency, instead of displaying a peak. Also, 2D geometric ratchets are easier to implement experimentally since these do not require carving very many inclined asymmetric grooves, as with a 1D potential ratchet [7]. Moreover, as pointed out above

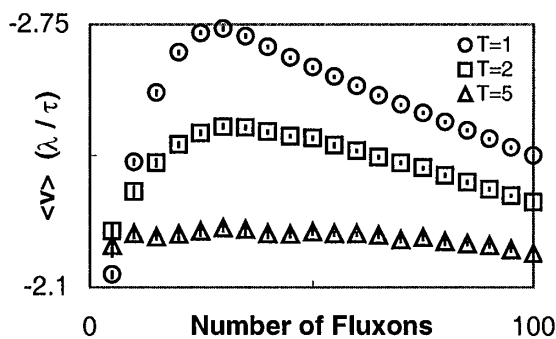


FIG. 3.  $\langle v \rangle$  versus the number of fluxons for several values of the temperature  $T$ .

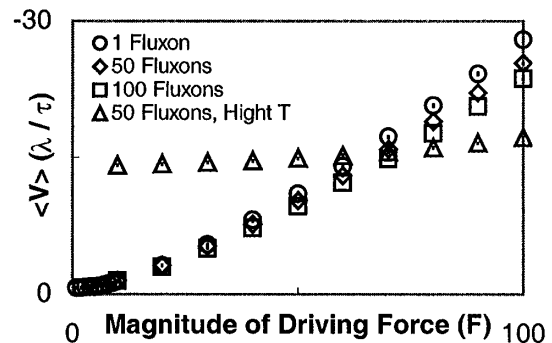


FIG. 4.  $\langle v \rangle$  versus magnitude  $F$  of the driving force. The number of fluxons for the low- $T$  ( $T = 5$ ) cases are 1 ( $\circ$ ), 50 ( $\diamond$ ), and 100 ( $\square$ ). 50 fluxons were used for the high- $T$  ( $T = 50$ ) curve ( $\triangle$ ).

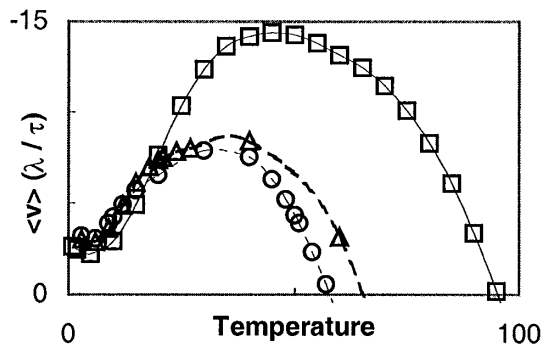


FIG. 5.  $\langle v \rangle$  versus  $T$  for different ratchet geometries, characterized by  $(S, P_{st})$ , where  $S$  is the slope with respect to  $x$ , and  $P_{st}$  is the spatial period of the sawteeth. The curves shown correspond to  $(1/3, 9)$  ( $\square$ ),  $(2/3, 9/2)$  ( $\triangle$ ), and  $(1, 3)$  ( $\circ$ ).

(Fig. 4),  $\langle v \rangle$  can be continuously tuned by varying  $F$ , for the 2D geometric ratchets. Furthermore, this type of 2D ratchet produces more robust transport since they lack the current inversion present in standard 1D ratchets [1].

*Concluding remarks.*—Superconducting devices using stochastic transport were studied because they provide a convenient way to move fluxons through channels. At nonzero temperatures, the asymmetric geometry of the ratchet sawteeth automatically converts applied ac inputs into a net dc motion of fluxons. Thus, the simulated device serves as an excellent fluxon rectifier. Our device could be easily made experimentally either by electron beam lithography, irradiation, evaporating layers, or by chemically etching a channel. The central channel would have very weak pinning, while the rest very strong pinning. By coupling two ratchets that rectify in opposite directions [see inset of Fig. 2(b) and [10]], fluxon *lenses* that could either 2(c) *disperse* or 2(d) *concentrate* fluxons in chosen regions of a sample can be created. More complex *fluxon optics* microdevices could be built similarly. Corners 2(e) can also be constructed. Such remarkable devices, and modifications of them, would allow the transport of fluxons along complicated nanofabricated channels: a microscopic network of fluxon channels in superconducting devices. This could be very useful to get rid of unwanted, trapped flux in SQUID magnetometers, and also to move fluxons along channels in devices [11]. These promising concepts are largely unexplored, and constitute an open and potentially useful area.

C. J. O. (J. F. W.) acknowledges support from the GSRP of the microgravity division of NASA (NSF-REU). We thank R. Riolo and the UM-CSCS for providing

computing resources. We acknowledge conversations with C. Doering, S. Field, A. Barabasi, and E. H. Brandt.

\*Corresponding author: nori@umich.edu

- [1] R. D. Astumian, *Science* **276**, 917 (1997); M. O. Magnasco, *Phys. Rev. Lett.* **71**, 1477 (1993); **72**, 2656 (1994); J. Prost *et al.*, *ibid.* **72**, 2652 (1994); C. R. Doering, W. Horsthemke, and J. Riordan, *ibid.* **72**, 2984 (1994); R. D. Astumian and M. Bier, *ibid.* **72**, 1766 (1994); L. P. Faucheux *et al.*, *ibid.* **74**, 1504 (1995); I. Derényi and T. Vicsek, *ibid.* **75**, 374 (1995); R. Bartussek, P. Reimann, and P. Hänggi, *ibid.* **76**, 1166 (1996); I. Derényi, C. Lee, and A. L. Barabási, *ibid.* **80**, 1473 (1998).
- [2] Applications of potential interest to biology are discussed in S. Leibler, *Nature (London)* **370**, 412 (1994); J. Maddox, *Nature (London)* **365**, 203 (1993); **368**, 287 (1994); **369**, 181 (1994).
- [3] F. Marchesoni, *Phys. Rev. E* **56**, 2492 (1997); *Phys. Rev. Lett.* **77**, 2364 (1996); F. Marchesoni, L. Gammaitoni, and A. R. Bulsara, *ibid.* **76**, 2609 (1996).
- [4] C. R. Doering, *Physica (Amsterdam)* **254A**, 1 (1998); *Nuovo Cimento Soc. Ital. Fis.* **17D**, 685 (1995); C. R. Doering *et al.*, *Chaos* **8**, 643 (1998); T. C. Elston and C. R. Doering, *J. Stat. Phys.* **83**, 359 (1996).
- [5] R. P. Feynman, R. B. Leighton, and M. Sands, *The Feynman Lectures on Physics* (Addison-Wesley, Reading, MA, 1966), Vol. I, Chap. 46.
- [6] I. Zapata *et al.*, *Phys. Rev. Lett.* **77**, 2292 (1996); **80**, 829 (1998); F. Falo *et al.*, *Europhys. Lett.* **45**, 700 (1999).
- [7] C. S. Lee, B. Jankó, I. Derényi, and A. L. Barabási [*Nature (London)* **400**, 337 (1999)] present independent work on ratchets (1D type instead of the 2D boundary-effect pump described here). J. W. Wambaugh *et al.* (unpublished) also performed independent work on 1D fluxon ratchets. Early work on asymmetric-shaped pinning traps can be found, e.g., in E. H. Brandt, *J. Low Temp. Phys.* **53**, 41 (1983).
- [8] F. Nori, *Science* **278**, 1373 (1996); C. Reichhardt *et al.*, *Phys. Rev. B* **53**, R8898 (1996); *ibid.* **52**, 10441 (1995); C. J. Olson *et al.*, *ibid.* **56**, 6175 (1997); *Phys. Rev. Lett.* **80**, 2197 (1998); **81**, 3757 (1998).
- [9] C. Reichhardt *et al.*, *Phys. Rev. B* **54**, 16108 (1996); **56**, 14196 (1997); **58**, 6534 (1998); **57**, 7937 (1998); *Phys. Rev. Lett.* **78**, 2648 (1997); **82**, 414 (1999).
- [10] Magnified color versions of the figures appear in <http://www-personal.engin.umich.edu/~nori/ratchet>.
- [11] *Applications of Superconductivity*, edited by H. Weinstock (Kluwer, Dordrecht, 1999); *SQUID Sensors*, edited by H. Weinstock (Kluwer, Dordrecht, 1996); *New Superconducting Electronics*, edited by H. Weinstock (Kluwer, Dordrecht, 1993); H. Weinstock, *Physica (Amsterdam)* **209C**, 269 (1993); *IEEE Trans. Magn.* **27**, 3231 (1991).